Production of like sign dileptons in *p-p* collisions through composite Majorana neutrinos

O. Panella*
Istituto Nazionale di Fisica Nucleare, Sezione di Perugia, Via A. Pascoli, I-06123 Perugia, Italy

C. Carimalo
Laboratoire de Physique Nucléaire et de Hautes Energies, IN2P3-CNRS Universités Paris VI/VII, 4 place Jussieu, F-75252, Paris Cedex 05, France

Y. N. Srivastava
Dipartimento di Fisica dell' Università e INFN, Sezione di Perugia, Via A. Pascoli, I-06123 Perugia, Italy and Northeastern University, Physics Department, Boston, Massachusetts 02155

(Received 8 March 1999; revised manuscript received 4 February 2000; published 12 June 2000)

The production of like-sign dileptons (LSD) in the high-energy lepton-number-violating ($\Delta L=+2$) reaction $pp\rightarrow 2$ jets$+l^+l^+$ ($l=e,\mu,\tau$), of interest for experiments to be performed at the forthcoming CERN Large Hadron Collider (LHC), is investigated in detail, taking up a composite model scenario in which the exchanged virtual *composite* neutrino is assumed to be a Majorana particle that couples to the light leptons via the SU(2)×U(1) gauge bosons through a magnetic type coupling ($\sigma_{\mu\nu}$). A helicity projection method is used to evaluate exactly the tree-level amplitudes of the contributing parton subprocesses ($2\rightarrow 4$), which allows one to take into account all exchange diagrams and occurring interferences. Numerical estimates of the corresponding signal cross section that implement kinematical cuts needed to suppress the standard model background are presented which show that in some regions of the parameter space the total number of LSD events is well above the background. Assuming nonobservation of the LSD signal it is found that LHC would exclude a composite Majorana neutrino up to ≈ 900 GeV (if one requires 10 events for discovery). The sensitivity of LHC experiments to the parameter space is then compared to that of the next generation of neutrinoless double beta decay ($\beta\beta_{0\nu}$) experiment, GENIUS, and it is shown that they will provide constraints of the same order of magnitude and will play a complementary role.

PACS number(s): 12.60.Rc, 13.15.+g, 13.85.Rm, 14.60.St

I. INTRODUCTION

Since the discovery of the Z^0 and $W^{\pm}$ gauge bosons [1] the standard model (SM) of electroweak interactions [2] based on the SU(2)×U(1) gauge group has scored an impressive record of experimental checks. However, some unexplained facts of the model, such as the mass hierarchy, the proliferation of elementary particles, and the total number of free parameters, have lead to the belief that it is only a low-energy manifestation of a yet unknown underlying fundamental theory, which would be free of the above theoretical difficulties. Therefore despite the enormous experimental success of the SM many alternative theories have been developed such as left-right symmetric models, composite models, supersymmetry, string theory, and grand unified models. The investigation of the effects predicted by the new theories that are absent in the standard theory is therefore very important since, were these effects to be experimentally observed, they would signal *new physics* unaccounted for by the SM. It is in this direction that a great portion of recent theoretical and experimental studies have been concentrated [3], and this is indeed the spirit of this work which deals with lepton-number-violating processes.

The conservation of the total lepton number (L) is one of the symmetries of the SM experimentally observed to hold true until now. In the SM with massless Dirac neutrinos processes with $\Delta L\neq 0$ are not possible. Violation of this symmetry is generally related to the existence of massive Majorana particles and many extensions of the SM contain L-violating interactions involving Majorana neutrinos. Left-right symmetric models for example contain right-handed Majorana neutrinos, with a mass that could be in the TeV range, and coupled to the light leptons via the right-handed gauge bosons (W_R, Z_R) [4]. Superstring generated E_6 models also have neutral Majorana leptons [5]. Finally Ref. [6] provides an example of a composite model with Majorana neutrals.

The effect which seems most promising with respect to showing violations of the lepton number is the neutrinoless double beta decay ($\beta\beta_{0\nu}$), a second order process where, in a nucleus, two protons (neutrons) undergo simultaneously a weak beta decay emitting two positrons (electrons) while the two neutrinos annihilate into the vacuum [3]:

$$A(Z+2)\rightarrow A(Z)+e^+e^+, \quad \Delta L=+2. \tag{1}$$

This process is only possible if the neutrino is a massive Majorana particle, and thus it is impossible within the SM. Experiments that search for such rare decay have long since been performed but always with negative results [7]. Currently the Heidelberg-Moscow $\beta\beta$ experiment at the Gran-

*Author to whom correspondence should be addressed. Electronic address: Orlando.Panella@PG.infn.it

Sasso laboratory in Italy provides the best experimental lower bound on the half-life of the process [8]

$$^{76}\mathrm{Ge}\rightarrow{}^{76}\mathrm{Se}+2\,e^{-},$$
$$T_{1/2}^{\beta\beta_{0\nu}}>5.7\times10^{25}\ \mathrm{yr}. \tag{2}$$

The proposed GENIUS double beta experiment (see Sec. VI), now under development, will either increase the lower bound on the half-life by two or three orders of magnitude or observe the decay. From the theoretical point of view, the strong bound on the half-life in Eq. (2) has been turned into a powerful tool to impose constraints on models of new physics which predict a nonzero amplitude for the $\beta\beta_{0\nu}$ decay [9]. Studies in this direction include: an investigation of new super-symmetric contributions from *R*-parity violating minimal supersymmetric standard model (MSSM) [10] which shows how constraints on parameters of the model from nonobservation of $\beta\beta_{0\nu}$ are stronger than those available from accelerator experiments; a detailed analysis of the contribution to $\beta\beta_{0\nu}$ from left-right symmetric models [11]; a study of the effective low-energy charged current lepton-quark interactions due to the exchange of heavy leptoquarks [12].

The present authors have, in a series of recent papers [13–15], investigated the contribution, to the neutrinoless double beta decay, of a heavy Majorana neutrino, arising from a composite model scenario in which the excited partner of the neutrino (the excited neutrino, $\nu^{\star}$) is assumed to be a Majorana particle. This study revealed that $\beta\beta_{0\nu}$ constraints are competitive, and in some regions of the parameter space, even more restrictive than those derived from high-energy direct search of excited particles [15,16]. This result led to consider the potential of the experiments to be performed at the forthcoming Large Hadron Collider (LHC) at CERN, with respect to the possibility of observing the production of like-sign dileptons (LSD) $l^{+}l^{+}$ or $l^{-}l^{-}$, $l=e,\mu,\tau$, in proton-proton collisions with an energy of 14 TeV in the center of mass frame

$$pp\rightarrow 2\mathrm{jets}+\mathrm{LSD},\quad \Delta L=+2. \tag{3}$$

In hadronic collisions LSD can be produced in quark-quark (antiquark-antiquark) scattering, through the elementary subprocess $W^{+}W^{+}\rightarrow l^{+}l^{+}$ (virtual *W*-boson fusion) as depicted in Fig. 1 where the dashed blob represents all contributing diagrams within a given model. As regards this mechanism of LSD production one can say that it is the high-energy analogue of the neutrinoless double beta decay which indeed proceeds through the same Feynman diagrams (see, for example, Ref. [15]). Figure 2(a) shows explicitly the Feynman diagram for the production of LSD through the exchange of a heavy Majorana neutrino (basic mechanism). In the case of quark-antiquark scattering in addition to the *W* fusion another mechanism must be considered that leads to LSD production: the direct production of a heavy Majorana neutrino via quark-antiquark annihilation $q\bar{q}'\rightarrow l^{+}N$ with the subsequent decay of the heavy neutrino $N\rightarrow l^{+}q\bar{q}'$ (annihilation mechanism). This is depicted in Fig. 2(b).

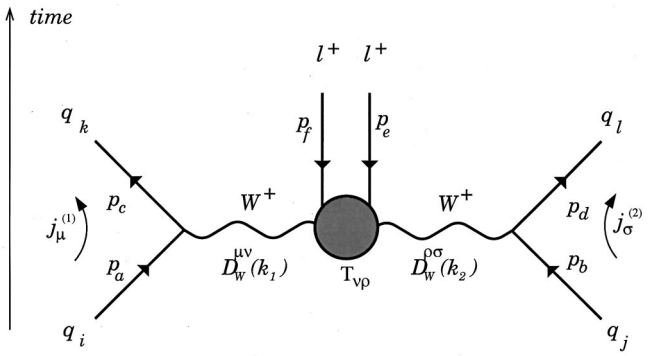

FIG. 1. Parton level mechanism for production of like-sign-dileptons (LSD) in high-energy hadronic collisions. The shaded blob contains all contributing diagrams for the virtual subprocess $W^{+}W^{+}\rightarrow l^{+}l^{+}$.

Production of LSD has been considered in the past by several authors and within the context of different models. In the left-right symmetric model, Keung and Senjanović [17] already in 1983 realized that the associate production of LSD with two hadronic jets would signal the annihilation of quark-antiquark pairs into the right-handed gauge boson of

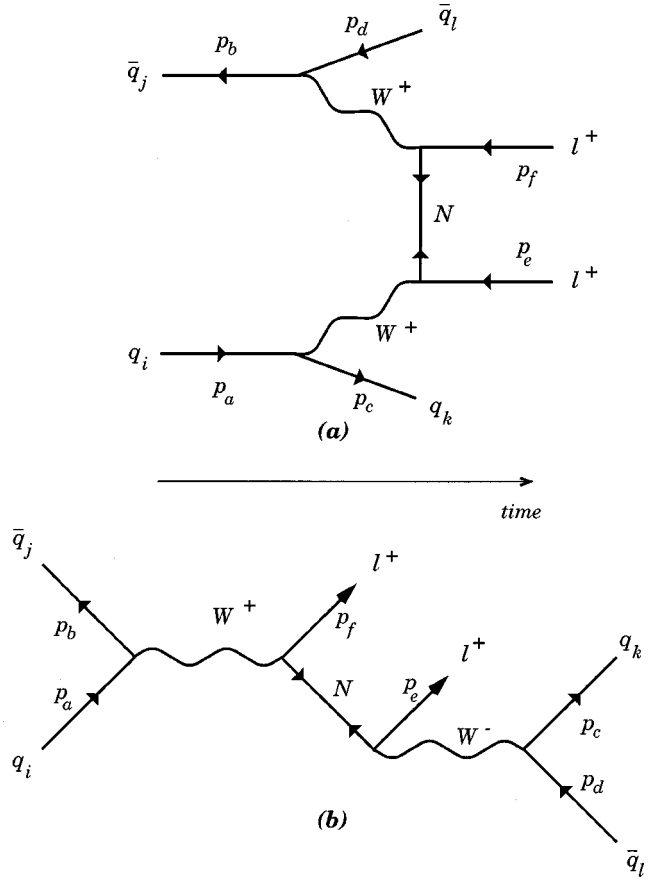

FIG. 2. Production of LSD through quark-antiquark scattering. There are here two interfering mechanisms to be considered (a) virtual W fusion, (b) $l^{+}N_l$ production via quark-antiquark annihilation with subsequent hadronic decay of the heavy neutrino $N_l\rightarrow l^{+}q\bar{q}$.

the model (W_R). Estimates were given for pp collisions at $\sqrt{s}=800$ GeV. The study of this model was later taken up to higher energies [Superconducting Super Collider (SSC) and LHC] by Datta, Guchait, and Roy in Ref. [18] where the authors indicated how to effectively reduce the SM background. Dicus, Karatas, and Roy [19] have studied LSD production at high-energy hadron colliders through the exchange of heavy right-handed Majorana neutrinos, without commitment to a specific model (beyond the SM). They used a γ_μ-type coupling and found the LSD signal detectable at the SSC while at the LHC the SM background would probably preclude detection. Two of the present authors [20] provided a rough estimate of the signal cross sections for $pp \rightarrow 2\text{jets}+\text{LSD}$ at LHC within the context of composite models (exchange of a heavy composite Majorana neutrino with a $\sigma_{\mu\nu}$-type coupling) using an equivalent W-boson approximation [21] (similar to the Weiszäcker-Williams approximation for the photon field) and integrating over the complete phase-space of the subprocess $W^+W^+ \rightarrow l^+l^+$. The result was that the signal could be observable at the LHC.

One remark should be made at this point that applies to all works just cited that have investigated LSD production in pp collisions. None of them deals, *at the same time*, with the two mechanisms of LSD production, i.e., W^+W^+ fusion and $q\overline{q}'$ annihilation. Indeed when dealing with $q\overline{q}'$ scattering both mechanisms must be considered and the corresponding amplitudes should be added coherently. In order to do so one needs a way of efficiently computing the amplitudes. In this paper it is done precisely so, calculating analytically the helicity amplitudes of the occurring tree-level diagrams and accounting thus for the interference term between the W^+W^+ fusion and the $q\overline{q}'$ annihilation.

Thus the goal of this paper is twofold: (i) to address the sensitivity of LHC experiments with respect to the parameters of the composite model effective Lagrangian and compare this to that of the next generation of double beta decay experiments now under development (GENIUS); (ii) to present a calculation of LSD production in pp collisions (via the exchange of a heavy composite Majorana neutrino) which goes beyond the approximations of Ref. [20] and which, in the case of $q\overline{q}'$ annihilation, includes coherently the two competing mechanisms.

The rest of the paper is organized as follows. In Sec. II the reader is briefly reminded of the effective Lagrangian describing the coupling of the excited neutrino with the electron and a comparison between recent bounds on the parameters from the low-energy $\beta\beta_{0\nu}$ experiment by the Heidelberg-Moscow Collaboration and those from high energy experiments performed by the DELPHI Collaboration at the CERN Large Electron Positron (LEP) Collider is presented. In Sec. III the amplitudes of the L-violating parton subprocesses are presented. Section IV contains (i) a description of the kinematical cuts applied with a short discussion of the background; (ii) our numerical results for the signal cross sections. In Sec. V the sensitivity to the parameter space of LHC is compared to that of GENIUS. Finally, Sec. VI contains the conclusions.

II. COMPOSITENESS AND EXISTING $\beta\beta_{0\nu}$ CONSTRAINTS

It is well known that one possible scenario of physics beyond the SM is one in which quarks and leptons are not elementary particles but possess an internal structure; i.e., they are bound states of, yet unknown, new constituents, generally referred to as *preons*, bound together by a new dynamical interaction. Theories that follow this path are called *composite models* and although many have been proposed [22] none has emerged as a new dynamically consistent theory. However, there are some model-independent consequences of the idea of compositeness which can be addressed without commitment to any specific model. These are (i) contact interactions between ordinary fermions, (ii) the existence of excited partners for quarks and leptons with masses of the order of the compositeness scale Λ_c. Phenomenologically these ideas have been studied via effective interactions [14,23]. In particular in this work, the case of excited neutrinos (N), is taken up and only the relevant coupling with the light electron are reviewed. Effective couplings between the heavy and light leptons (or quarks) have been proposed, using weak isospin (I_W) and hypercharge (Y) conservation [24]. Assuming that such states are grouped in $\mathrm{SU}(2)\times\mathrm{U}(1)$ multiplets, since light fermions have $I_W=0,1/2$ and electroweak gauge bosons have $I_W=0,1$, only multiplets with $I_W \leqslant 3/2$ can be excited in the lowest order perturbation theory. Also, since none of the gauge fields carry hypercharge, a given excited multiplet can couple only to a light multiplet with the same Y. Conservation of the electromagnetic current forces the transition coupling of heavy-to-light fermions to be of the magnetic moment type respect to any electroweak gauge bosons [24]. In fact, a vector (γ_μ) transition coupling between the ordinary electron e and its excited partner E mediated by the $\vec{W}^\mu$ and B^μ gauge fields, would result in an electromagnetic current of the type $j^\mu_{\text{e.m.}} \approx \overline{\psi}_E \gamma^\mu \psi_e$ which would not be conserved due to the different masses of excited and ordinary fermions (as it is expected that $m_E \gg m_e$). The $\mathrm{SU}(2)\times\mathrm{U}(1)$ symmetry forces then the tensor structure ($\sigma_{\mu\nu}$) to the transition coupling also in the charged and neutral weak currents.

Restrict here to the first family and consider spin-1/2 excited states grouped in multiplets with $I_W=1/2$ and $Y=-1$ (the so called homodoublet model [23]),

$$L=\begin{pmatrix} N \\ E \end{pmatrix} \tag{4}$$

which can couple to the light left-handed multiplet

$$l_L=\begin{pmatrix} \nu_L \\ e_L \end{pmatrix}=\frac{1-\gamma_5}{2}\begin{pmatrix} \nu \\ e \end{pmatrix} \tag{5}$$

through the gauge fields $\vec{W}^\mu$ and B^μ. The relevant interaction is written [24] in terms of two *new* independent coupling constants f and f':

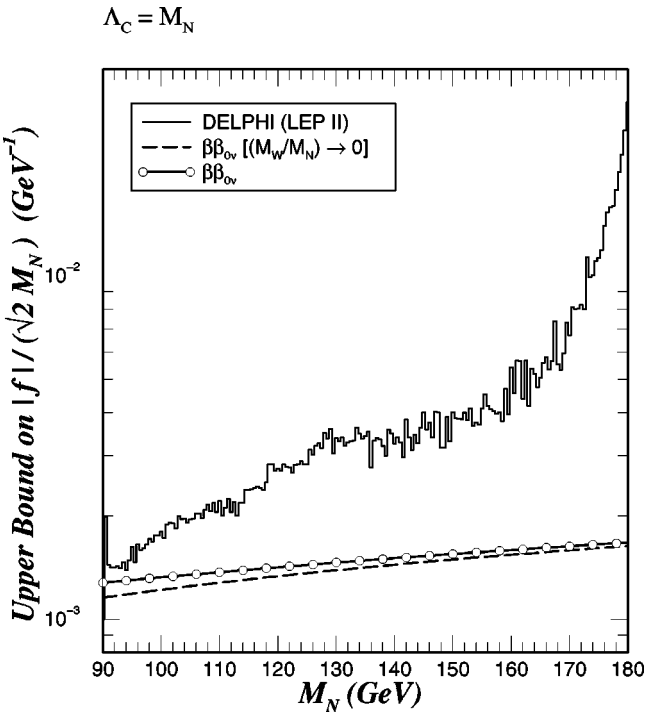

FIG. 3. Comparison between the $\beta\beta_{0\nu}$ and the LEP II upper bound on the quantity $|f|/(\sqrt{2}M_N)$ as a function of the heavy neutrino mass M_N, with the choice $\Lambda_c = M_N$. Regions above the curves are excluded. The dashed curve is the $\beta\beta_{0\nu}$ bound of Eq. (10), while the solid-circle curve includes numerical effects of terms of higher order in M_W/M_N as discussed in Ref. [16].

$$\mathcal{L}_{int} = \frac{gf}{\Lambda_c}\bar{L}\sigma_{\mu\nu}\frac{\vec{\tau}}{2}l_L\cdot\partial^\nu\vec{W}^\mu + \frac{g'f'}{\Lambda_c}\left(-\frac{1}{2}\bar{L}\sigma_{\mu\nu}l_L\right)\cdot\partial^\nu B^\mu + \text{H.c.}, \tag{6}$$

where $\vec{\tau}$ are the Pauli SU(2) matrices, g and g' are the usual SU(2) and U(1) gauge coupling constants, and the factor of $-1/2$ in the second term is the hypercharge of the U(1) current. This effective Lagrangian is widely used in the literature to predict production cross sections and decay rates of the excited particles [23,25,26]. In terms of the physical gauge fields the interaction Lagrangian describing the coupling of the heavy excited neutrino with the light electron is therefore

$$\mathcal{L}_{\text{eff}} = \left(\frac{gf}{\sqrt{2}\Lambda_c}\right)\left\{\left(\bar{N}\sigma^{\mu\nu}\frac{1-\gamma_5}{2}e\right)\partial_\nu W^+_\mu\right\} + \text{H.c.} \tag{7}$$

In the analysis carried out in Refs. [13,14] it was assumed that the excited neutrino is a Majorana particle with mass M_N, expected to be of the order of the compositeness scale Λ_c, which would then contribute to the neutrinoless double beta decay.

It should be emphasized how this scenario differs considerably from the more usual one of the left-right symmetric model where a SU(2) singlet Majorana neutrino couples to the charged leptons via a right-handed W gauge boson (W_R) and $(V+A)$ coupling [27]. Here (and in Refs. [13,14]) instead the heavy composite Majorana neutrino belongs to a SU(2) doublet [see Eq. (4)] and interacts with the charged lepton via the standard model W gauge boson (left handed) with a tensor coupling $[\sigma_{\mu\nu}(1-\gamma_5)]$.

In Ref. [14] the half-life of the $\beta\beta_{0\nu}$ mediated by a heavy composite Majorana neutrino (coupling to the charged lepton via the SM W gauge boson and with tensor coupling) was calculated and found to be given by

$$T^{-1}_{1/2} = \left(\frac{f}{\Lambda_c}\right)^4 \frac{m_A^8}{M_N^2}|\mathcal{M}_{FI}|^2\frac{G_{01}}{m_e^2}, \tag{8}$$

where $m_A = 0.85$ GeV is a parameter entering the nuclear form factors, $\mathcal{M}_{FI} = -5.45\times10^{-2}$ is a nuclear matrix element, m_e is the electron mass, and $G_{01} = 6.4\times10^{-15}$ yr^{-1} is a phase space integral. Combining this result with the non-observation of the decay ($T_{1/2} > T^{\text{lower bound}}_{1/2}$) one obtains a constraint on the parameters of the model

$$\left|\frac{f}{\Lambda_c}\right| < M_N^{1/2}\left(\frac{m_e^2}{m_A^8}\right)^{1/4}\frac{[G_{01}\,T^{\text{lower bound}}_{1/2}]^{-1/4}}{|\mathcal{M}_{FI}|^{1/2}}. \tag{9}$$

Using the current experimental lower bound on the half-life of the ^{76}Ge decay provided by the Heidelberg-Moscow $\beta\beta$ experiment, the following constraint on the parameters f, Λ_c, M_N appearing in Eq. (7) is deduced:[1]

$$|f| \leqslant 8.03\frac{\Lambda_c}{1\text{ TeV}}\left(\frac{M_N}{1\text{ TeV}}\right)^{1/2}. \tag{10}$$

This double beta bound on compositeness can be compared with bounds on the same parameters from high-energy experiments performed at the Large Electron Positron (LEP) collider, phase II. The DELPHI Collaboration has reported [28] on a search for excited leptons in e^+e^- collisions at $\sqrt{s} = 183$ GeV, where both the single and double production mode were studied. It should be emphasized that the analysis in Ref. [28] was carried out using the same effective Lagrangian that was considered in Refs. [13,15], cf. Eq. (7), so that it makes sense to compare the corresponding bounds. In Fig. 3 the bound of Eq. (10) is plotted against the exclusion curve of the DELPHI Collaboration [28], and one can see that for masses above $\approx$90 GeV the double beta bound is more constraining, i.e., it excludes a portion of parameter phase space still allowed by the DELPHI exclusion plot.[2]

[1]This is an updated constraint respect to that of Ref. [15] where a previous value of the half-life was used.

[2]It should be noted that the ALEPH Collaboration has also recently published results of a search for compositeness at LEP I. In Ref. [29] bounds on the compositeness scale, in particular regarding the same excited neutrino couplings discussed here, are reported. Choosing $f = f' = 1$ a neutrino mass-dependent lower bound on Λ_c is found which is about 16 TeV at $M_N = \mathcal{O}(10\text{ GeV})$ while it drops down to 4 TeV at the maximum value of M_N explored of 80 GeV. This result is not directly comparable to Eq. (10) since this was derived within the hypotesis $M_N >> M_W$ [15]. Assuming $|f| = 1$, Eq. (10) gives $\Lambda_c \geqslant 0.12$ TeV at $M_N = 1$ TeV.

This result prompted the present authors to study the potential of the LHC with respect to the same type of lepton-number-violating processes, with an emphasis on comparing its sensitivity with that of the next generation of double beta decay experiments.

One comment is finally due on the the related issue of the detectability of the charged partner of the heavy composite Majorana neutrino, the so called excited electron E. The heavy electron E is currently being searched for in experiments performed at high-energy facilities which look for its direct production and/or indirect effects in electron-positron colliders (LEP at CERN) and/or electron-proton colliders (ep collider HERA at DESY). The most recent and stringent bounds on the mass of the heavy electron E is from studies of indirect (propagator) effects in $e^+e^-\to\gamma\gamma$ where the E is exchanged in the t channel. The ALEPH Collaboration reports $m_E>250$ GeV [30]. The single production in electron-proton collisions ($ep\to E+X$), gives also bounds of the same order of magnitude: $m_E>200$ GeV [31]. As regards the production of excited electrons E at hadron colliders it was realized some time ago [32] that these can be copiously produced via contact interactions (CTs), arising from a new *strong* preon dynamics, as opposed to the gauge interactions (G) being discussed here. One process that could be looked upon at the LHC to estimate E production through gauge interactions is $u\bar{d}\to W^*\to \nu E$ with the subsequent decay $E\to e\gamma$. This would give a signature $pp\to e\nu\gamma+X$ whose cross section is expected to be of the same order of magnitude of those described here. However, this goes beyond the scope of the present work, and should be the object of further investigation.

The following section deals with the calculation of the lepton number violating processes in pp collisions described by the diagrams of Figs. 1 and 2. They have been carried out with a choice of the parameters that satisfies the bounds from $\beta\beta_{0\nu}$ just discussed.

III. AMPLITUDES OF L-VIOLATING PARTON SUBPROCESSES

In the following the helicity amplitudes for parton subprocesses that contribute to production of LSD via the exchange (or production) of a heavy Majorana composite neutrino are presented. The effective interaction used is that of Eq. (7). Considering for the moment only the first family, three different types of processes should be distinguished:

$$\begin{aligned}&\text{(i) } uu\to dd+l^+l^+,\\ &\text{(ii) } u\bar{d}\to d\bar{u}+l^+l^+,\\ &\text{(iii) } \bar{d}\bar{d}\to\bar{u}\bar{u}+l^+l^+.\end{aligned}\tag{11}$$

The amplitudes are written using the following definitions of propagator factors:

$$\begin{aligned}1/A&=[(p_a-p_c)^2-M_W^2][(p_b-p_d)^2-M_W^2],\\ 1/B&=[(p_a-p_d)^2-M_W^2][(p_b-p_c)^2-M_W^2],\end{aligned}\tag{12}$$

$$\begin{aligned}1/\tilde{A}&=[(p_a+p_b)^2-M_W^2+iM_W\Gamma_W]\\ &\quad\times[(p_c+p_d)^2-M_W^2+iM_W\Gamma_W],\\ C&=(p_a-p_c-p_e)^2-M_N^2,\\ D&=(p_a-p_c-p_f)^2-M_N^2,\\ E&=(p_a-p_d-p_e)^2-M_N^2,\\ F&=(p_a-p_d-p_f)^2-M_N^2,\\ \tilde{C}&=(p_c+p_d+p_f)^2-M_N^2+iM_N\Gamma_N,\\ \tilde{D}&=(p_c+p_d+p_e)^2-M_N^2+iM_N\Gamma_N.\end{aligned}\tag{13}$$

The width of the heavy composite neutrino Γ_N is of course a quantity which depends on the free parameters of the particular model that is being considered here, $|f|$, Λ_c, and M_N, and has been the object of discussion in the literature [32,26]. Typically the width of excited leptons (quarks) receives contributions from the gauge interactions of Eq. (7) and from contact terms arising from novel *strong* preon interactions [26].[3] In order to keep the numerical computations of cross-sections presented in the following reasonably simple, a constant value of $\Gamma_N=70$ GeV has been adopted, which is a somewhat average value in the mass range considered.

Define also the quantities

$$\begin{aligned}s(m,n)&=s(p_m,p_n)=\bar{u}_+(p_m)u_-(p_n),\\ t(m,n)&=t(p_m,p_n)=\bar{u}_-(p_m)u_+(p_n),\end{aligned}\tag{14}$$

which are given by

$$\begin{aligned}s(m,n)&=-2\sqrt{E_mE_n}G_{mn},\\ t(m,n)&=+2\sqrt{E_mE_n}F_{mn},\end{aligned}\tag{15}$$

with

$$\begin{aligned}G_{mn}&=\cos(\theta_m/2)\sin(\theta_n/2)\,e^{+i(\phi_m-\phi_n)/2}\\ &\quad-\sin(\theta_m/2)\cos(\theta_n/2)\,e^{-i(\phi_m-\phi_n)/2},\\ F_{mn}&=(G_{mn})^*.\end{aligned}\tag{16}$$

Let the tensor $T_{\mu\nu}$ describe the virtual sub-process $W^\star W^\star\to l^+l^+$ [Fig. 2(a)], while the tensor $\tilde{T}_{\mu\nu}$ describes the virtual subprocess $(W^\star)^+\to l^+l^+(W^\star)^-$ appearing in the diagram of Fig. 2(b). $J_{a,c}$ and $\bar{J}_{b,d}$, are the quark (antiquark) currents that couple in the t channel to the virtual gauge bosons of the standard model [Fig. 2(a)] while $\tilde{J}_{a,b}$ and $\tilde{J}^*_{c,d}$, are the in-

[3]It is to be noted, however, that these contact terms while contributing to the total width of the excited neutrino cannot contribute to the production of LSD via the diagrams discussed in this work.

coming and outgoing currents of the $q\overline{q'}$ pair that couples in the s channel to the W bosons [Fig. 2(b)].

$$J^{\mu}_{a,c}=\overline{u}(p_c)\,\gamma^{\mu}\frac{1-\gamma_5}{2}u(p_a),$$

$$\overline{J}^{\mu}_{b,d}=\overline{v}(p_b)\,\gamma^{\mu}\frac{1-\gamma_5}{2}v(p_d),$$

$$\tilde{J}^{\mu}_{a,b}=\overline{v}(p_b)\,\gamma^{\mu}\frac{1-\gamma_5}{2}u(p_a), \tag{17}$$

$$(\tilde{J}^{\mu}_{c,d})^{*}=\overline{u}(p_c)\,\gamma^{\mu}\frac{1-\gamma_5}{2}v(p_d).$$

The amplitudes are (unitary gauge)

(i) $\underline{U_iU_j\to D_kD_l+l^+l^+}$

$$\mathcal{M}=\mathcal{K}\{V^{*}_{U_iD_k}V^{*}_{U_jD_l}A\,[J^{\mu}_{(a,c)}\,T_{\mu\nu}\,J^{\nu}_{(b,d)}] - V^{*}_{U_iD_l}V^{*}_{U_jD_k}B\,[(p_c\leftrightarrow p_d)]\}, \tag{18}$$

(ii) $\underline{U_i\overline{D}_j\to D_k\overline{U}_l+l^+l^+}$

$$\mathcal{M}(WW-\text{fusion}) =\mathcal{K}(V_{U_iD_k})^{*}(V_{U_lD_j})^{*}\,[A\,J^{\mu}_{(a,c)}\,T_{\mu\nu}\,\overline{J}^{\nu}_{(b,d)}],$$

$$\mathcal{M}(q\overline{q'}-\text{annihilation}) =\mathcal{K}(V_{U_iD_j})^{*}(V_{U_lD_k})^{*}\,[\tilde{A}\,\tilde{J}^{\mu}_{(a,b)}\,\tilde{T}_{\mu\nu}(\tilde{J}^{\nu}_{(c,d)})^{*}], \tag{19}$$

(iii) $\underline{\overline{D}_i\overline{D}_j\to\overline{U}_k\overline{U}_l+l^+l^+}$

$$\mathcal{M}=\mathcal{K}\{V^{*}_{U_kD_i}V^{*}_{U_lD_j}A\,[\overline{J}^{\mu}_{(a,c)}\,T_{\mu\nu}\,\overline{J}^{\nu}_{(b,d)}] - V^{*}_{U_lD_i}V^{*}_{U_kD_j}B[(p_c\leftrightarrow p_d)]\}, \tag{20}$$

where U_i denotes a positively charged quark (up-type) while D_i dentotes a negatively charged one (down-type). The quantities $V_{U_iD_j}$ are the elements of the CKM mixing matrix. Of course the annihilation diagram of Fig. 2(a) comes in only in quark-antiquark scattering. In processes (i) and (iii) the part of the amplitude depending on the factor B is due to the diagrams obtained exchanging the final state quarks. In the framework of the effective Lagrangian [see Eq. (7)] as discussed in Sec. II, it is found

$$T_{\mu\nu}=\overline{u}(p_e)\left[\frac{\sigma_{\mu\rho}\sigma_{\nu\sigma}}{C}+\frac{\sigma_{\nu\sigma}\sigma_{\mu\rho}}{D}\right]\frac{1-\gamma_5}{2}v(p_f) \times(p_a-p_c)^{\rho}(p_b-p_d)^{\sigma},$$

$$\tilde{T}_{\mu\nu}=\overline{u}(p_e)\left[\frac{\sigma_{\mu\rho}\sigma_{\nu\sigma}}{\tilde{C}}+\frac{\sigma_{\nu\sigma}\sigma_{\mu\rho}}{\tilde{D}}\right]\frac{1-\gamma_5}{2}v(p_f) \times(p_a+p_b)^{\rho}(p_c+p_d)^{\sigma},$$

$$\mathcal{K}=\frac{g^4}{4}\left(\frac{f}{\Lambda_c}\right)^2 M_N. \tag{21}$$

Because of the chiral nature of the couplings involved, the calculation is particularly simple if performed in the helicity basis [33]. In the massless approximation only one helicity amplitude is nonzero. The following result is found:

(i) $\underline{U_iU_j\to D_kD_l+l^+l^+}$

$$\mathcal{M}=4\,\mathcal{K}\,s(a,b)\Bigg\{(V_{U_iD_k})^{*}(V_{U_jD_l})^{*}\,A\,t(a,c)t(d,b) \times\left[\frac{s(e,a)s(b,f)}{C}-\frac{s(f,a)s(b,e)}{D}\right] -(V_{U_iD_l})^{*}(V_{U_jD_k})^{*}\,B\,t(a,d)t(c,b) \times\left[\frac{s(e,a)s(b,f)}{E}-\frac{s(f,a)s(b,e)}{F}\right]\Bigg\}, \tag{22}$$

(ii) $\underline{U_i\overline{D}_j\to D_k\overline{U}_l+l^+l^+}$

$$(WW-\text{fusion}):\quad \mathcal{M}=+4\,\mathcal{K}(V_{U_iD_k})^{*}(V_{U_lD_j})^{*} \times A\,s(a,d)t(a,c)t(d,b) \times\left\{\left[\frac{s(e,a)s(d,f)}{C}-\frac{s(f,a)s(d,e)}{D}\right]\right\}, \tag{23}$$

$$(q\overline{q'}-\text{annihilation}):$$

$$\mathcal{M}=-4\,\mathcal{K}(V_{U_iD_j})^{*}(V_{U_lD_k})^{*}\tilde{A}\,t(a,b)s(a,d)t(d,c) \times\left\{\left[\frac{s(e,a)s(d,f)}{\tilde{C}}-\frac{s(f,a)s(d,e)}{\tilde{D}}\right]\right\}, \tag{24}$$

(iii) $\underline{\overline{D}_i\overline{D}_j\to\overline{U}_k\overline{U}_l+l^+l^+}$

$$\mathcal{M}=4\,\mathcal{K}\,s(c,d)\Bigg\{(V_{U_kD_i})^{*}(V_{U_lD_j})^{*}\,A\;t(a,c)t(d,b) \times\left[\frac{s(e,c)s(d,f)}{C}-\frac{s(f,c)s(d,e)}{D}\right]+(V_{U_lD_i})^{*}(V_{U_kD_j})^{*} \times B\;t(a,d)t(c,b)\left[\frac{s(e,d)s(c,f)}{E}-\frac{s(f,d)s(c,e)}{F}\right]\Bigg\}. \tag{25}$$

The above simple analytic form of the amplitudes is also very easy to implement in a code for numerical applications,

since the quantities $s(p_i,p_j)$ and $u(p_i,p_j)$ are just functions of the energies and angles of the particle's momenta; see Eqs. (15) and (16).

IV. DISCUSSION AND RESULTS

Before giving details of numerical calculations of the signal cross section and discussing the results one should be reminded that there are processes of the standard model that also lead to LSD production and are thus sources of background to the signal. This question was already considered in Refs. [18,19]. An immediate source of background comes from the subprocesses $uu \to ddW^+W^+$, $u\bar{d} \to d\bar{u}W^+W^+$, $\bar{d}\bar{d} \to \bar{u}\bar{u}W^+W^+$ and similar ones involving higher-generation quarks and antiquarks, each W subsequently decaying into $l\nu_l$. The corresponding overall reaction $pp \to 2\,\text{jets}\, l\nu_l\, l\nu_l$ can mimic the signal when the total missing P_T carried away by the neutrinos is small. As shown in Ref. [19], that background can be most efficiently reduced to a percent of fb in LHC conditions, which will be shown to be at the same level of the signal, in some regions of the parameter space, or even well below the latter in other regions. This background reduction is accomplished by limiting the missing P_T of neutrinos, that is, requiring a ''P_T conservation'' which is actually a characteristic of the signal.

As also observed in Refs. [18,19], a copious and more dangerous source of standard-model background seems to be due to $t\bar{t}$ production from gluon and quark initial states. In that process, one has the decay chains $t \to bW^+$, $W^+ \to l\nu_l$ on one side and $\bar{t} \to \bar{b}W^-$, $\bar{b} \to \bar{c}l\nu_l$, $W^- \to qq'$ on the other side. For LHC conditions, that reaction leads to a total production of about 4×10^6 LSD per year. Here again, a limitation of missing P_T together with the condition of large P_T leptons allow one to reduce substantially that background. The additional requirement of lepton isolation further reduces the background. But while the two requirements of missing P_T limitation and lepton isolation will certainly eliminate two other similar backgrounds coming from direct $c\bar{c}$ and $b\bar{b}$ production, that of $t\bar{t}$ production seems to remain, according to Refs. [18,19], at a level which might jeopardize measurement of the signal at LHC.

At this point, it is worth noticing that within the standard model one can observe in pp collisions not only events with like-sign dileptons of a given species ($e^\pm e^\pm$, $\mu^\pm\mu^\pm$, $\tau^\pm\tau^\pm$), but also events with ''hybrid'' like-sign dileptons (HLSD) such as $e^\pm\mu^\pm$, $e^\pm\tau^\pm$, $\mu^\pm\tau^\pm$, with practically the same production rate for all these events since the W's decay into any $l\nu_l$ final state at the same rate. Thus, one can get an idea on the amount of standard-model LSD background and eventually make appropriate subtraction by comparing, under given kinematical constraints, LSD production with HLSD production. At LHC, it would be most probably a comparison between $\mu^\pm\mu^\pm$, $\tau^\pm\tau^\pm$ production and $\mu^\pm\tau^\pm$ production. Said differently, once appropriate kinematical cuts performed, any significant difference between LSD production and HLSD production would signal lepton number violating processes such as those here considered. However, let us remark that a no-deviation result could not rule out new physics models allowing for lepton mixing.

In any case let us remark that an analysis of the background dedicated specifically to the LHC experimental conditions, and perhaps more complete than that presented in Refs. [18,19], is necessary (including in particular a detailed calculation of the amplitude of the processes involved), and will be the matter of a forthcoming work. Here the estimate of the background given in Ref. [19] is assumed:

$$\sigma_{\text{background}} = 3\times10^{-2}\ \text{fb}. \tag{26}$$

In order to compare the signal cross-section with Eq. (26) kinematical cuts as discussed in Ref. [19] are used. The following selection criteria are needed in order to ensure lepton and jet identification:

$$\begin{aligned} |\eta_{\text{lep}}| &< 4 \quad p_T(\text{lep}) > 5\ \text{GeV}, \\ |\eta_{\text{jet}}| &< 4 \quad p_T(\text{jet}) > 20\ \text{GeV}. \end{aligned} \tag{27}$$

The signal cross sections are obtained by folding the square of the amplitudes with the four-particle phase-space and the parton distribution functions

$$\begin{aligned} d\sigma = \int dx_a dx_b \frac{1}{1+\delta_{ij}} &[f_i(x_a,Q^2) f_j(x_b,Q^2) + x_a \leftrightarrow x_b] \\ &\times \frac{1}{2\hat{s}} |\mathcal{M}|^2 (2\pi)^4\, \delta^4\left(p_a + p_b - \sum_{m=1}^{4} p_m\right) \\ &\times \frac{1}{2}\left(1 - \frac{\delta_{kl}}{2}\right) \prod_{n=1}^{4} \frac{d^3\boldsymbol{p}_n}{(2\pi)^3 2E_n}, \end{aligned} \tag{28}$$

where $\hat{s} = x_a x_b S$ is the squared center of mass energy of the parton collision and the factor $(1/2)(1-\delta_{kl}/2)$ accounts for the presence of the two identical fermions (l^+l^+) and the possibly identical quarks U_k, U_l ($\bar{U}_k, \bar{U}_l$) in the final state. The distribution functions are those of set 1.1 of Duke-Owens (updated version of set 1) as described in Ref. [34] with $\Lambda_{QCD} = 177$ MeV/c. $\sqrt{S} = 14$ TeV has been used while the scale Q^2 is fixed at the value $Q^2 = \hat{s}$. With a proper choice of the transverse axis the phase-space reduces to a nine-dimensional integration that is performed with the well known VEGAS [35] routine which is based on a Monte Carlo algorithm. This allows easy implementation of kinematical cuts as described above. As regards the $u\bar{d}$ process the interference between the WW-fusion and annihilation mechanisms is naturally taken into account since the two (complex) amplitudes are summed before squaring.

In Figs. 4–6 the integrated cross section with the parameter $|f| = 1$, i.e., $\sigma_1 = \sigma(|f| = 1)$ is given. As $\mathcal{M} \propto f^2$, the total cross section for other values of $|f|$ can be easily recovered ($\sigma = |f|^4 \times \sigma_1$). Keeping fixed $|f| = 1$ there are other two parameters on which our signal rate is dependent: Λ_c and M_N. In order to sample different regions of the parameter space two cases have been considered. Case (a) $\Lambda_c = 1$ TeV, and case (b) $\Lambda_c = M_N$.

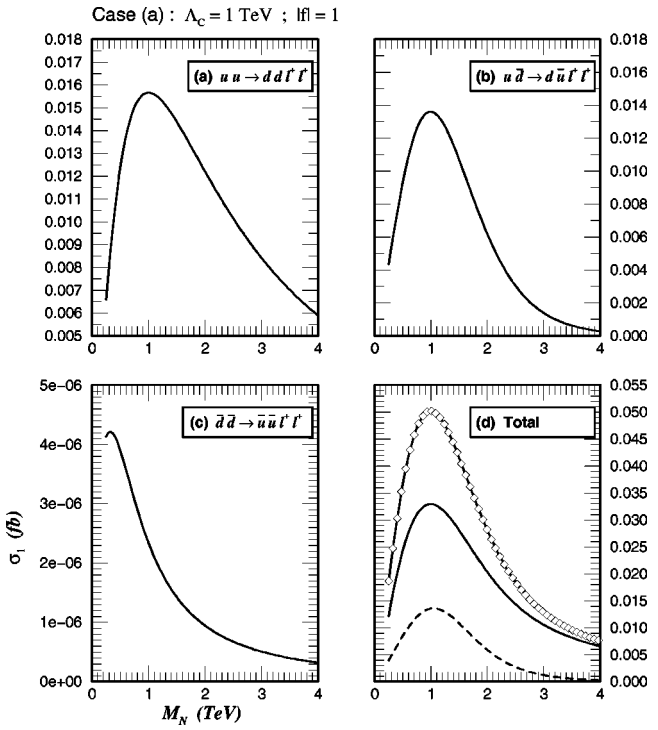

FIG. 4. Cross section normalized to $|f|=1$, i.e., $\sigma_1=\sigma/|f|^4$ with the choice $\Lambda_c=1$ TeV. (a)$uu\to dd+l^+l^+$, (b) $u\bar{d}\to d\bar{u}+l^+l^+$, (c) $\bar{d}\bar{d}\to\bar{u}\bar{u}+l^+l^+$, (d) the *solid* line is the sum of the contributions from Figs. 4(a)–4(c) including factorizable corrections according to Eqs. (A1),(A2); the *dashed* line is the process $u\bar{d}\to s\bar{c}+l^+l^+$ according to Eq. (A3). Finally the *solid-diamond* line in (d) is the total cross section σ_1 including the sum of the subleading contributions reported in Fig. 5.

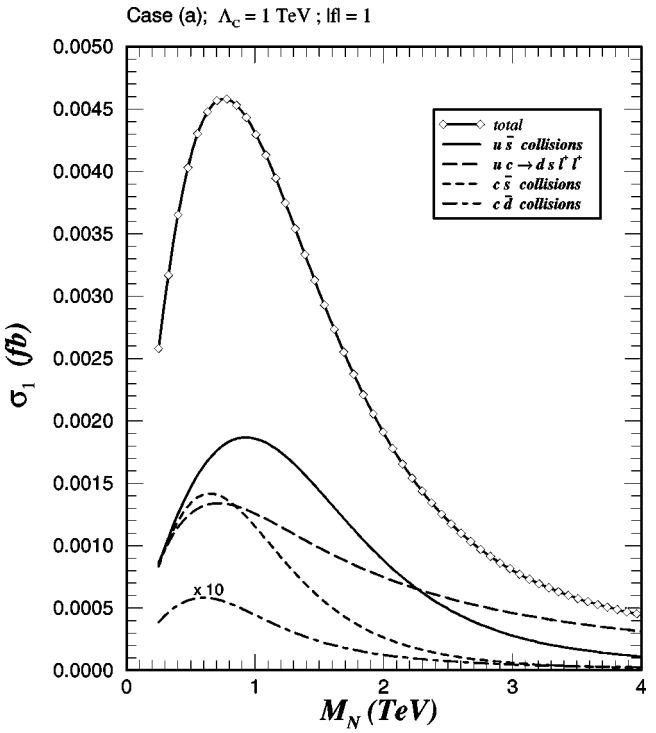

FIG. 5. Subleading processes: the *solid* line is the sum of $u\bar{s}$ collisions Eqs. (A4) and (A5); the long-dashed line is the process $uc\to ds+l^+l^+$; the dashed line is the sum of $c\bar{s}$ collisions, Eqs. (A6) and (A7); the dot-dashed line is the the sum of $c\bar{d}$ collisions, Eqs. (A8) and (A9), scaled by a factor of 10. Finally the *solid-diamond* line is the total contribution to σ_1 of the above processes.

Case (a) is shown in Fig. 4 where cross sections corresponding to the three subprocesses of the first quark family, cf. Eq. (11), are plotted versus the mass of the excited Majorana neutrino M_N [Figs. 4(a)–4(c)]. Since the subprocess $\bar{d}\bar{d}\to\bar{u}\bar{u}+l^+l^+$ is weighted by sea-quark distribution functions it is totally negligible relative to the other two. In Fig. 4(d) the *total cross section* is plotted versus M_N including contributions from other subprocesses with second generation quarks, (c,s) as described in the appendix. Some of these subprocesses are, however, weighted by off-diagonal elements of the CKM mixing matrix and therefore give only small corrections. The shape of the curves as a function of M_N is clearly understood since the only dependence on the new parameters is of the type[4]

$$\sigma\sim\left(\frac{|f|}{\Lambda_c}\right)^4 M_N^2\int\sum_K\frac{1}{(K^2-M_N^2)^2+\theta(K^2)(M_N\Gamma_N)^2}, \tag{29}$$

where K are different momenta flowing in the Majorana propagator. Thus in case (a), $\sigma\to 0$ as $M_N\to 0$ while $\sigma\sim M_N^{-2}$ as $M_N\to\infty$, and there is an intermediate region with a maximum. There is a mass interval from $M_N=250$ GeV up to $M_N\approx 3$ TeV where σ_1 is bigger than the lowest measurable cross section of 10^{-2} fb that corresponds to one event per year given the luminosity $\mathcal{L}_0=100$ fb^{-1} (integrated over one year) planned at LHC. For example, the total signal cross section σ_1 is at most about 5×10^{-2} fb, which is at the same level (though bigger) of the background [Eq. 26], and would only give five events per year. It seems therefore that, *with this particular choice of parameters* [case (a) $\Lambda_c=1$ TeV, $|f|=1$], the lepton number violating signal due to the composite Majorana neutrino would hardly be measurable, unless a better set of kinematical cuts is found that enhances the absolute value of the signal rate while reducing still further the background. However one should keep in mind the dependence on the parameter $|f|$, which in Fig. 4 has been fixed to $|f|=1$. Since the signal cross section is proportional to $|f|^4$ even a slightly larger value of $|f|$ could increase sensibly the signal cross section.

Case (b) is shown in Fig. 6 with the same notation as in Fig. 4. Again the subprocess $\bar{d}\bar{d}\to\bar{u}\bar{u}+l^+l^+$ [Fig. 6(c)] is

[4]It should be remarked that this is only true within the approximation of a constant width Γ_N for the heavy neutrino. Taking into account the dependence of Γ_N with the new physics parameters $|f|$, M_N, and Λ_c (and those pertaining to contact terms) could modify, to some extent, the contibution of the quark-antiquark scattering. However, as pointed out in Ref. [26], Γ_N receives the largest contribution from contact terms which are independent of $|f|$.

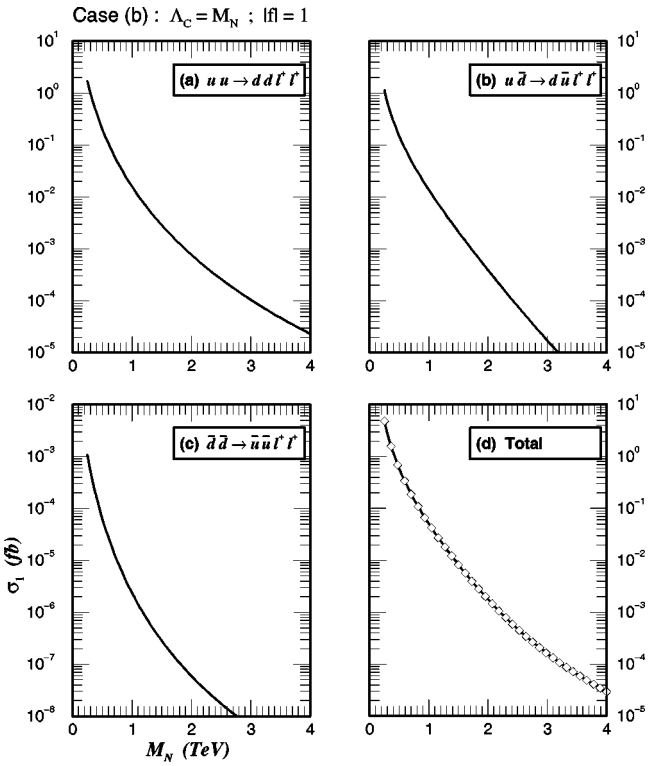

FIG. 6. Same as in Fig. 4 but with the choice $\Lambda_c = M_N$. As explained in the text the different shape of the cross section σ_1 as function of M_N with respect to Fig. 4 is because $\sigma_1 \propto \Lambda_c^{-4}$. Thus fixing $\Lambda_c = M_N$ gives of course a different function of M_N than choosing $\Lambda_c = 1$ TeV. The solid-diamond line in (d) again describes the total σ_1 as done in Fig. 4.

totally negligible relative to the other two. The different shape of the cross section σ_1 as a function of M_N is of course due to the choice $\Lambda_c = M_N$, which according to Eq. (29) gives roughly $\sigma_1 \sim M_N^{-6}$ as $M_N \to \infty$ while $\sigma_1 \sim M_N^{-2}$ as $M_N \to 0$. Thus σ_1 is strongly enhanced with respect to case (a) for values of $M_N < 1$ TeV, while for $M_N > 1$ TeV it will be severely decreased. The cross section σ_1 will be measurable in the mass interval $M_N = 250$ GeV (400 events/yr) up to $M_N \approx 1.4$ TeV (1 event/yr). This portion of the parameter space has therefore the potential of giving rise to a signal with a substantially higher number of events with respect to the background, at least up to $M_N = 850$ GeV (10 events/yr).

The sensitivity of numerical results on different parametrizations of the parton distribution functions (PDFs) has been studied in detail. Calculations concerning the dominant processes have been performed using three other, more recent, sets of PDFs, namely: CTEQ (2pM) [36], Martin-Roberts-Stirling (MRS) (G) [37] and Glück-Reya-Voyt 1994 harmonic oscillator (GRV94) HO [38]. In order to understand better possible dependencies on PDFs the scale of the average x probed by the processes under consideration has been estimated by evaluating:

$$\langle x_a x_b \rangle = \frac{\int dx_a dx_b \, (x_a x_b) \dfrac{d\sigma}{dx_a dx_b}}{\int dx_a dx_b \dfrac{d\sigma}{dx_a dx_b}} \tag{30}$$

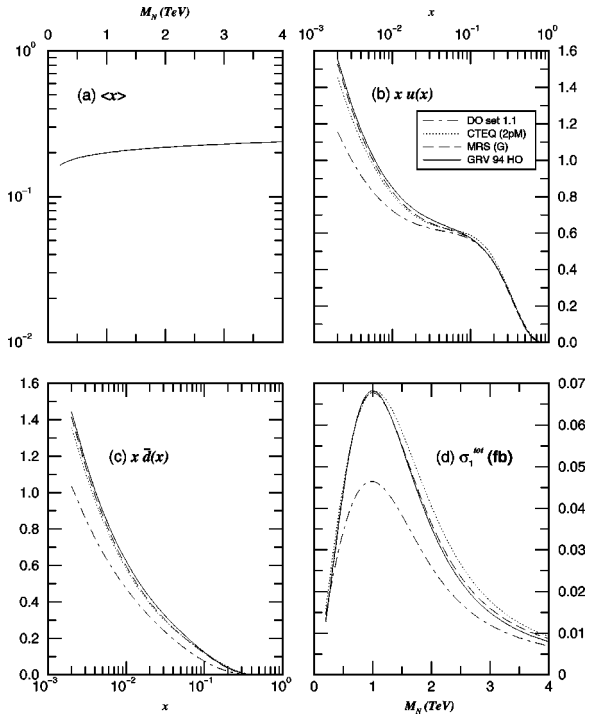

FIG. 7. (a) Average x as a function of M_N calculated for the process $uu \to dd$ + LSD with the parton distribution functions of DO set 1.1; (b) u quark distribution function at $Q = 1$ TeV for the different parametrizations chosen; (c) same as in (b) but for $\bar{d}$; (d) the total integrated cross section including the processes $uu \to dd$ + LSD, $u\bar{d} \to d\bar{u}$ + LSD, and $u\bar{d} \to s\bar{c}$ + LSD. $\sigma_{\rm tot}$ is not including the subleading processes reported in Fig. 5. These were shown to give corrections of the order of 10%.

and then taking

$$\langle x \rangle \sim \sqrt{\langle x_a x_b \rangle}. \tag{31}$$

As shown in Fig. 7(a) the LSD signal probes x values in the region of $x \approx 0.2$ over the full range of heavy neutrino masses considered.

Figures 7(b) and 7(c) show a comparison of the parton distribution functions of DO, CTEQ, MRS, and GRV. The latter have a considerably larger $\bar{d}(x)$ relative to DO down to the region of $x \approx 0.2$ while the $u(x)$ distribution function differs, in this very same region, only by a few percent. One expects therefore that using CTEQ, MRS, and GRV will change only slightly the cross-section of the process $uu \to dd$ + LSD while that of $u\bar{d} \to d\bar{u}$ + LSD process will be enhanced by somewhat larger factors. This is indeed verified by the numerical calculation.

In Table I sample numerical results for the integrated cross section of $uu \to dd$ + LSD are shown at different values of the heavy neutrino mass M_N. One finds that the cross section of the uu process with CTEQ, MRS, and GRV, relative to the calculation performed with DO, varies up to $\approx +6\%$ for $M_N = 1$ TeV. The same comparison is shown in Table II for the process $u\bar{d} \to d\bar{u}$ + LSD. In this case a much stronger sensitivity is found, as expected. At $M_N = 1$ TeV the

TABLE I. Sensitivity of numerical results with respect to the different parton distribution parametrizations. Comparing the cross section of the subprocess $uu \to dd + l^{\pm} l^{\pm}$. Case (a) $\Lambda_c = 1$ TeV. Cross sections are expressed in fb.

M_N (GeV)	DO set 1.1	CTEQ 2pM	MRS (G)	GRV 94 HO
500	0.12712×10^{-1}	0.13667×10^{-1}	0.13491×10^{-1}	0.12743×10^{-1}
1000	0.16176×10^{-1}	0.17333×10^{-1}	0.17254×10^{-1}	0.15994×10^{-1}
2000	0.12501×10^{-1}	0.13351×10^{-1}	0.13421×10^{-1}	0.12220×10^{-1}

average value obtained with CTEQ, MRS, and GRV is $\approx +65\%$ higher than that of D0.

In Fig. 7(d) the total integrated cross section (not including the subleading processes discussed in Fig. 5) is compared between the different set of PDFs. One finds that at $M_N = 1$ TeV (where the cross section reaches its maximum value) CTEQ, MRS, and GRV predict a value larger by about 55% with respect to the DO result. This difference of course is very important as far as one is interested in the total number of signal events but, as it will be shown, changes only by about 10% the bounds on the compositeness parameters discussed on Sec. V. One might say (since the CTEQ, MRS, and GRV predictions are all very close), that the DO prediction is rather conservative.

Finally it should be remarked that the discussion, so far, has been quite general with respect to the lepton flavor and applicable to all three of them but (LSD$= l^{\pm} l^{\pm}$, $l = e, \mu, \tau$) at the LHC, muons will be the leptons most easily detected while the other lepton flavors will be detectable but with lower efficiencies [39]. For this reason the numerical results presented here refer to only one lepton generation.

V. COMPARING THE LHC VS THE GENIUS POTENTIAL

This section contains a comparative discussion of the constraints on the parameters $|f|$, M_N, Λ_c that could be derived by the nonobservation of the L-violating signals discussed in the previous section at the high-energy LHC experiments as opposed to those deriving from the nonobservation of low-energy neutrinoless double beta decay experiments, present (Heidelberg-Moscow) and next-generation (GENIUS). The new $\beta\beta_{0\nu}$ GENIUS experiment, (GErmanium-detectors in liquid NItrogen as shielding in an Underground Setup) [40], has the potential to improve by orders of magnitude the lower bound on the $\beta\beta_{0\nu}$ decay half-life. Monte Carlo simulations have shown (for a 1 ton setup) that in one (four) year(s) of measurement the lower bound will be increased, respectively, to [40,41]

$$T^{0\nu}_{1/2} > 5.8 \times 10^{27} \text{ yr}, \quad [\text{one year}],$$

$$T^{0\nu}_{1/2} > 2.3 \times 10^{28} \text{ yr} \quad [\text{four years}].$$

Figures 8 and 9 show the upper bound on the parameter $|f|$ as function of the heavy neutrino mass M_N for the two cases (a) and (b) defined in the previous section. The curves concerning the $\beta\beta_{0\nu}$ bound are based on formulas that can be found in Ref. [16] which, relative to Eq. (10) above, include small correction terms of order $\mathcal{O}(M_W/M_N)$. The LHC curves are found using the numerical cross-sections presented in the previous section, requiring 10 events/yr as a criterion for discovery of the L-violating signal, and assuming an integrated luminosity of $\mathcal{L}_0 = 100$ fb^{-1} as before. Thus nonobservation of the signal at LHC means that $|f|^4 \sigma_1(M_N, \Lambda_c)\, \mathcal{L}_0 < 10$, which is translated into a constraint on $|f|$ that is the corresponding LHC upper bound to that in Eq. (10) from $\beta\beta_{0\nu}$:

$$|f| < \left(\frac{10}{\sigma_1 \mathcal{L}_0} \right)^{1/4}. \tag{32}$$

One remark is due here as regards the sensitivity to different sets of parton distribution functions. In Figs. 8 and 9 the LHC curve corresponding to the cross section σ_1^{tot} which includes the subleading terms discussed in Fig. 5 and found with the DO parametrization is the thick dot-dashed line. The other thin lines dot-dashed, dotted, long-dashed, and solid, are, respectively, the DO, CTEQ, MRS, and GRV bounds corresponding to the cross section σ_1^{tot} of Fig. 7(d) (all without subleading terms). Comparing the two dot-dashed lines one concludes that the inclusion of subleading terms gives corrections which are smaller than (or at most comparable to) the indeterminacy due the PDFs. The fact that the CTEQ, MRS, and GRV sets of PDFs give somewhat larger cross sections relative to DO, though important as regards the number of signal events and the signal to background ratio, is numerically less evident in Figs. 8 and 9 as here the LHC

TABLE II. Sensitivity of numerical results with respect to the different parton distribution parametrizations. Comparing the cross section of the subprocess $u\bar{d} \to d\bar{u} + l^{\pm} l^{\pm}$. Case (a) $\Lambda_c = 1$ TeV.

M_N (GeV)	DO set 1.1	CTEQ 2pM	MRS (G)	GRV 94 HO
500	0.11390×10^{-1}	0.15779×10^{-1}	0.12992×10^{-1}	0.13811×10^{-1}
1000	0.13617×10^{-1}	0.20878×10^{-1}	0.23133×10^{-1}	0.24700×10^{-1}
2000	0.65991×10^{-2}	0.12706×10^{-1}	0.11379×10^{-1}	0.10284×10^{-1}

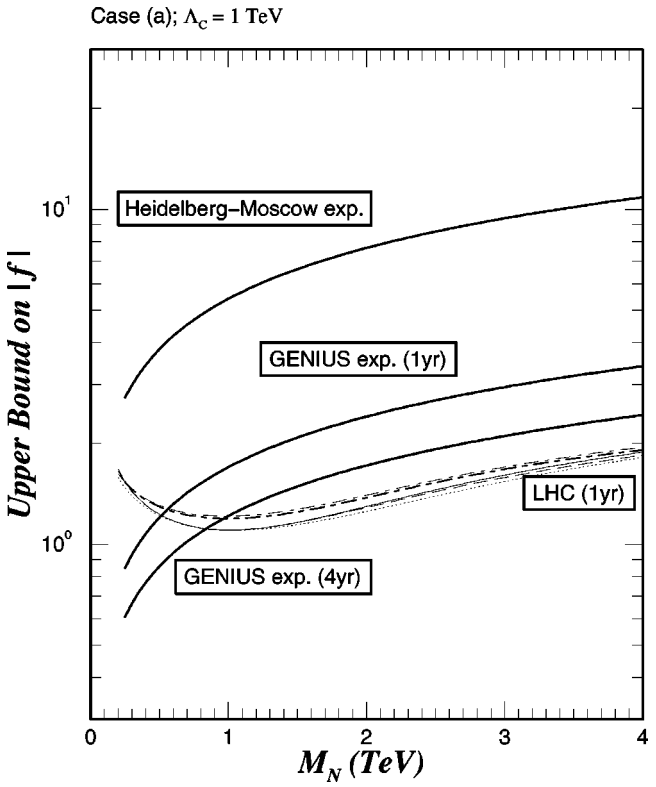

FIG. 8. Sensitivity of LHC vs current and next generation (GENIUS) double beta experiments to the compositeness parameters. Case (a) $\Lambda_c=1$ TeV. Nonobservation of the signal excludes regions above the curves. If no signal will be observed both LHC and GENIUS will be able to get upper bounds on $|f|$ stronger by almost an order of magnitude with respect to the present Heidelberg Moscow bound. The thick solid lines are the $\beta\beta_{0\nu}$; the thick dot-dashed line is the LHC bound with DO set 1.1 parametrization and $\sigma_1^{\rm tot}$ of Fig. 4(d) which includes the subleading terms of Fig. 5; the thin lines are the bounds corresponding to Fig. 7(d), DO (dot-dashed), CTEQ (dotted), MRS (long dashed), and GRV (solid). There is a region where the LHC bound is weaker than the GENIUS-1 yr bound $M_N<550$ GeV (DO), 500 GeV (CTEQ, MRS, and GRV) while for $M_N>550\,(500)$ GeV the LHC bound is stronger. The LHC bound is weaker than that of GENIUS-4 yr for $M_N<1000$ GeV (DO), 820 GeV (CTEQ, MRS, and GRV) while for $M_N>1000\,(820)$ GeV the LHC bound is stronger.

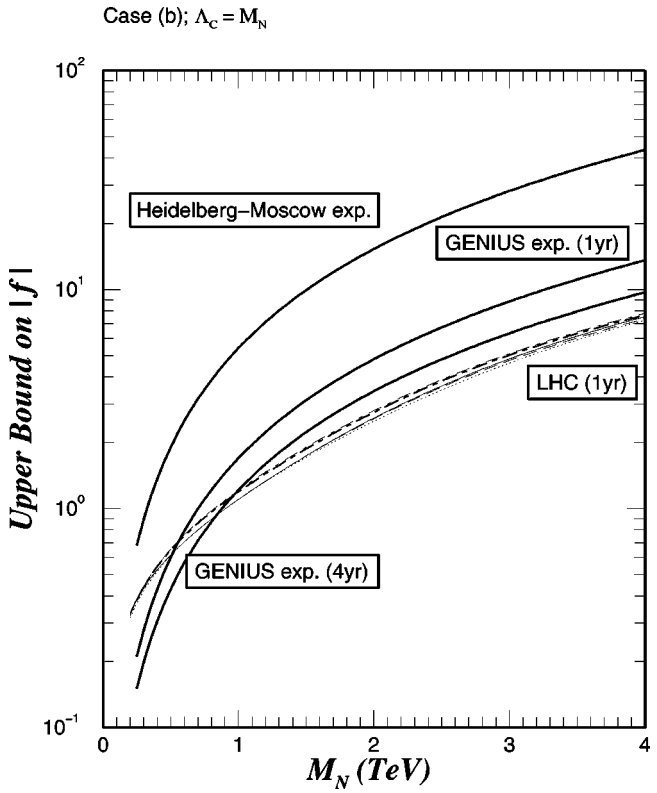

FIG. 9. Same as in Fig. 8 but with $\Lambda_c=M_N$. Also here regions above the curves are excluded. Here the shape of the LHC exclusion plot is similar to that of $\beta\beta_{0\nu}$. The values of M_N at which the LHC curves cross those of GENIUS are the same as in Fig. 8.

curves are obtained through Eq. (32) where σ_1 enters with a power of 1/4, and thus a change of a factor 1.5 in σ_1 gives a change in the bound on $|f|$ within 10%.

From Figs. 8 and 9 one can infer lower bounds on the composite neutrino mass (or equivalentely the compositeness scale) by assuming the dimensionless coupling $|f|\sim\mathcal{O}(1)$. For case (a), Fig. 8, one obtains the bounds shown in Table III while in Table IV the corresponding bounds for case (b), Fig. 9, are given. One comment is in order here. The LHC curve in Fig. 8 has a different behavior for $M_N<1$ TeV as compared to those of the $\beta\beta_{0\nu}$. This is due to the fact that as $M_N\to 0$, $\sigma_1\to 0$ and thus the LHC upper bound on $|f|$ becomes weaker and weaker. This does not happen in the $\beta\beta_{0\nu}$ whose squared amplitude behaves as $|\mathcal{M}_{\beta\beta_{0\nu}}|^2\sim M_N^{-2}$ [15] and at lower masses gives a bigger effect and therefore a stronger constraint. It is for this reason that Table III, for case (a), does not show a lower bound on M_N for LHC. In case (b) if $|f|\sim\mathcal{O}(1)$ GENIUS (1 yr) can exclude Majorana composite neutrinos up to a mass of $M_N\sim 700$ GeV, while LHC (with DO) and GENIUS (4 yr) can go up to about 850 GeV (the LHC bound is 930 GeV if using CTEQ, MRS, or GRV). It is important to realize that the nonaccelerator, low-energy, GENIUS-4yr experiment has the potential to probe the compositeness scale into the TeV region.

At this point the reader should be made aware that investigations of the same type of effective Lagrangians for com-

TABLE III. Lower bound on M_N for case (a) [$\Lambda_c=1$ TeV, $|f|=1$]. The bounds are derived from the nonobservation of neutrinoless double beta decay ($\beta\beta_{0\nu}$) at the current (Heidelberg-Moscow) experiment and for the prospected GENIUS experiment after 1 and 4 years of running [40]. At LHC nonobservation of the LSD signal would not imply a lower bound on the composite neutrino mass because of the different shape of the exclusion plot. See Fig. 8.

Experiment	Exp. constraint	Lower bound on M_N (GeV)
Heidelberg-Moscow	$T_{1/2}>5.7\times10^{25}$ yr	$M_N>\sim 10$
GENIUS 1 yr	$T_{1/2}>6.0\times10^{27}$ yr	$M_N>\sim 350$
GENIUS 4 yr	$T_{1/2}>2.3\times10^{28}$ yr	$M_N>\sim 700$
LHC	$N_{\rm events}<10$	

TABLE IV. Lower bound on M_N for case (b) [$\Lambda_c = M_N$, $|f| = 1$]. The bounds are derived from the nonobservation of neutrinoless double beta decay ($\beta\beta_{0\nu}$) at the current (Heidelberg-Moscow) experiment and for the prospected GENIUS experiment after 1 and 4 years of running [40] and from nonobservation of the LSD signal at LHC (less than 10 events in one year). See Fig. 9.

Experiment	Exp. constraint	Lower bound on M_N (GeV)
Heidelberg-Moscow	$T_{1/2} > 5.7\times10^{25}$ yr	$M_N > \sim 320$
GENIUS 1 yr	$T_{1/2} > 6.0\times10^{27}$ yr	$M_N > \sim 700$
GENIUS 4 yr	$T_{1/2} > 2.3\times10^{28}$ yr	$M_N > \sim 900$
LHC	$N_{\text{events}} < 10$	$M_N > \sim 850$ (DO) $> \sim 930$ (CTEQ,MRS,GRV)

positeness within the context of LHC experiments have already been reported in the literature. In particular while the production of excited quarks at LHC has been investigated both via magnetic type gauge (G) interactions and contact terms (CT) [32], the production of excited *leptons* has however been considered *only through* CT and a mass sensitivity of up to about 4–5 TeV is found [32]. This work is therefore the first report concerning excited leptons at LHC within the context of magnetic type gauge interactions, and, while the discovery limit derived for contact terms [14,32] cannot be directly compared with the constraints derived in Refs. [13–15] from the nonobservation of $\beta\beta_{0\nu}$ (that were based on gauge interactions G), the discovery limit for LHC reported here (M_N up to 850 GeV) can be directly compared with that of $\beta\beta_{0\nu}$ as done explicitly in Table IV and Figs. 8 and 9.

Finally it is worthwhile to note the complementary role that accelerator (LHC) and nonaccelerator experiments (GENIUS) can have. Figures 8 and 9 show explicitly that, in both cases (a) and (b), while for low masses the $\beta\beta_{0\nu}$ bound is more restrictive there is always a crossing point where the LHC constraint becomes stronger, though of the same order of magnitude.

VI. CONCLUSIONS

In this work the production of like-sign dileptons (LSD) via the exchange of a heavy composite Majorana neutrino in pp collisions has been studied in detail at LHC energies. The coupling of the Majorana neutrino is assumed to be a gauge interaction of the magnetic moment type ($\sigma_{\mu\nu}$). The helicity amplitudes have been presented and the resulting cross-sections within kinematical cuts, needed to suppress the SM background down to the fb level, are reported. Regions of the parameter space are pinned down where the signal is well above the estimated background ($\Lambda_c = M_N, |f| \sim 1, M_N < 850$ GeV). However, a study of the background specifically dedicated to the LHC experimental conditions would certainly be of help towards a better understanding of the lepton number violating processes discussed here. The comparison of the LHC potential with respect to observing L-violating processes with that of the new generation of the non-accelerator type $\beta\beta_{0\nu}$ experiment, GENIUS, shows how the two approaches, high- vs low-energy, do play a complementary role.

The approach developed here to discuss LSD production via composite Majorana neutrinos at LHC is being extended to other models of physics beyond the SM which provide L-violating interactions. The results of these analyses will be reported elsewhere.

One final remark is to be added concerning the interplay of low- vs high-energy facilities with respect to the study of lepton-number violation. The class of diagrams that give rise to $\Delta L = \pm 2$ processes discussed in this work could also trigger lepton-number-violating rare kaon decays such as $K^+ \to \pi^- e^+ e^+$. At the Frascati Φ factory, DAΦNE [42] (presently under commissioning), these decays could either be observed or, otherwise, the corresponding bounds on the branching ratios are susceptible to be strengthened. The current bound on the branching ratio for the ($\Delta L = -2$) K^+ decay is $\text{Br}(K^+ \to \pi^- e^+ e^+) < 1.0\times10^{-8}$ [23], while the sensitivity of the KLOE experiment [43] to be performed at DAΦNE could reach the level of 10^{-9}; the KLOE experiment might thus provide insights on lepton-number-violating interactions beyond the standard model. Work along these lines is in progress.

ACKNOWLEDGMENTS

The authors would like to thank M. Espirito-Santo, of the DELPHI Collaboration, for providing the data histogram plotted in Fig. 3. O.P. would like to acknowledge useful discussions with the experimental colleagues of the Compact Muon Solenoid (CMS) Collaboration, L. Servoli, G. M. Bilei, and M. Biasimi. C.C. acknowledges support by a grant from the Istituto Nazionale di Fisica Nucleare of Italy (INFN), that allowed his stay in Perugia, where this work was completed. He is also indebted to Z. Ajaltouni (ALEPH Collaboration), F. Fleuret, and S. Jan (ATLAS Collaboration) for useful discussions. This project is partially supported by the EEC-TMR Program, Contract No. CT98-0169.

APPENDIX A: LIST OF PARTON SUBPROCESSES

A list of all subprocesses leading to the production of LSD within the first two families of quarks follows.

(i) Quark scattering, $U_i U_j \to D_k D_l + l^+ l^+$,

$(k=l)$	$(k\neq l)$
$\boldsymbol{uu \to dd[ss] + l^+ l^+}$	$\boldsymbol{uu \to ds + l^+ l^+}$
$cc \to ss\ [dd] + l^+ l^+$	$cc \to ds + l^+ l^+$
$uc \to ss\ [dd] + l^+ l^+$	$\boldsymbol{uc \to ds + l^+ l^+}$.

(ii) Quark antiquark scattering ($U_i \bar{D}_j \to D_k \bar{U}_l + l^+ l^+$):

$$\boldsymbol{u\bar{d} \to d\bar{u}[d\bar{c}, s\bar{u}, s\bar{c}] + l^+ l^+}$$
$$\boldsymbol{u\bar{s} \to d\bar{c}[d\bar{u}, s\bar{u}, s\bar{c}] + l^+ l^+}$$
$$c\bar{s} \to s\bar{c}\ [s\bar{u}, d\bar{c}, d\bar{u}] + l^+ l^+$$
$$c\bar{d} \to s\bar{u}\ [s\bar{c}, d\bar{c}, d\bar{u}] + l^+ l^+ \ .$$

(iii) Antiquark scattering ($\bar{D}_i\bar{D}_i \to \bar{U}_k\bar{U}_l + l^+l^+$):

$(k=l)$	$(k\neq l)$
$\bar{d}\bar{d}\to\bar{u}\bar{u}\,[\bar{c}\bar{c}\,]+l^+l^+$	$\bar{d}\bar{d}\to\bar{u}\bar{c}+l^+l^+$
$\bar{s}\bar{s}\to\bar{c}\bar{c}\,[\bar{u}\bar{u}\,]+l^+l^+$	$\bar{s}\bar{s}\to\bar{u}\bar{c}+l^+l^+$
$\bar{d}\bar{s}\to\bar{u}\bar{u}\,[\bar{c}\bar{c}\,]+l^+l^+$	$\bar{d}\bar{s}\to\bar{c}\bar{u}+l^+l^+$.

Numerical results reported in Figs. 4(d) and 6(d) contain contributions from some of the processes listed above.

The following equations (A1)–(A9) have been adopted to estimate the contribution of the subprocesses due to second family partons. Note that in this section, and in numerical computations, the complex phases of the elements of the CKM mixing matrix have been neglected, assuming $V_{ij}^* = V_{ij}$, as only the first two generations are being considered.

Processes initiated by two *sea* partons and not receiving contribution from the annihilation diagram have not been considered since Figs. 4(c) and 6(c) show that they are clearly negligible. As regards quark scattering only two cases have been considered; subprocesses initiated by uu and uc collisions, i.e., with at least one u-quark in the initial state.

uu initiated subprocesses: the processes $uu\to dd+l^+l^+$, $uu\to ds+l^+l^+$, and $uu\to ss+l^+l^+$ are factorized as follows

$$|\mathcal{M}_{uu\text{-initiated}}|^2=\left[1+2\left|\frac{V_{us}}{V_{ud}}\right|^2+\left|\frac{V_{us}}{V_{ud}}\right|^4\right]\times|\mathcal{M}_{uu\to dd+l^+l^+}|^2, \tag{A1}$$

the additional factor of 2, in the equation above, accounts for the fact that the process $uu\to ds+l^+l^+$ does not contain identical quarks in the final state as opposed to the processes $uu\to dd+l^+l^+$ and $uu\to ss+l^+l^+$ and thus for it Eq. (28) applies with $k\neq l$.

Quark-antiquark scattering subprocesses have been divided into

$\underline{u\bar{d}}$ collisions: the processes $u\bar{d}\to[d\bar{u},s\bar{u},d\bar{c}]+l^+l^+$ are factorized as

$$|\mathcal{M}_{u\bar{d}\text{-initiated}}|^2=\left[1+\left|\frac{V_{us}}{V_{ud}}\right|^2+\left|\frac{V_{dc}}{V_{ud}}\right|^2\right]\times|\mathcal{M}_{u\bar{d}\to d\bar{u}+l^+l^+}|^2; \tag{A2}$$

the process $u\bar{d}\to s\bar{c}+l^+l^+$, does not factorize as above due to the fact that the *WW* fusion and the annihilation diagram come in with different factors of the elements of the CKM matrix

$$|\mathcal{M}_{u\bar{d}\to s\bar{c}+l^+l^+}|^2=\left|\frac{V_{us}V_{dc}}{V_{ud}^2}\mathcal{M}_{u\bar{d}\to d\bar{u}+l^+l^+}^{(WW\text{-fusion})}+\frac{V_{cs}}{V_{ud}}\mathcal{M}_{u\bar{d}\to d\bar{u}+l^+l^+}^{(u\bar{d}\text{-annihil})}\right|^2 \tag{A3}$$

[see Eq. (23]. It turns out to be numerically the most important subprocess, between those containing second family partons. It gives a contribution which is roughly equal to that of $uu\to dd+l^+l^+$ and $u\bar{d}\to d\bar{u}+l^+l^+$, accounting thus for about 30% of the total σ_1 reported in Fig. 4.

$\underline{u\bar{s}}$ collisions: the processes $u\bar{s}\to[s\bar{u},d\bar{u},s\bar{c}]+l^+l^+$ can be factorized as

$$|\mathcal{M}_{u\bar{s}\text{-initiated}}|^2=\left(\frac{V_{us}}{V_{ud}}\right)^4\left[1+\left|\frac{V_{ud}}{V_{us}}\right|^2+\left|\frac{V_{cs}}{V_{us}}\right|^2\right]\times|\mathcal{M}_{u\bar{d}\to d\bar{u}+l^+l^+}|^2, \tag{A4}$$

and using the fact the within the set of parton densities used here (set 1.1 of Duke and Owens [34]), $\bar{u}(x)=\bar{d}(x)=\bar{s}(x)$, the cross section for $u\bar{s}$ initiated collisions can be simply obtained from $\sigma_1(u\bar{d}\to d\bar{u}+l^+l^+)$ by multiplying it with the above CKM factor which is $0.10\approx 10\%$; the process $u\bar{s}\to d\bar{c}+l^+l^+$ does not factorize as in the above equation and must be considered separately (it is shown in Fig. 5):

$$\mathcal{M}_{u\bar{s}\to d\bar{c}+l^+l^+}=\left|\frac{V_{cs}}{V_{ud}}\mathcal{M}_{u\bar{d}\to d\bar{u}+l^+l^+}^{(WW\text{-fusion})}+\frac{V_{us}V_{dc}}{(V_{ud})^2}\mathcal{M}_{u\bar{d}\to d\bar{u}+l^+l^+}^{(u\bar{d}\text{-annihil})}\right|^2. \tag{A5}$$

$\underline{c\bar{s}}$ collisions: the processes $c\bar{s}\to[s\bar{c},s\bar{u},d\bar{c}]+l^+l^+$ can be factorized as

$$\begin{aligned}|\mathcal{M}_{c\bar{s}\text{-initiated}}|^2&=\left(\frac{V_{cs}}{V_{ud}}\right)^4\left[1+\left|\frac{V_{us}}{V_{cs}}\right|^2+\left|\frac{V_{cd}}{V_{cs}}\right|^2\right]\times|\mathcal{M}_{u\bar{d}\to d\bar{u}+l^+l^+}|^2,\\&=\left[1+\left|\frac{V_{us}}{V_{cd}}\right|^2+\left|\frac{V_{cs}}{V_{cd}}\right|^2\right]\times|\mathcal{M}_{c\bar{s}\to d\bar{c}+l^+l^+}|^2,\end{aligned} \tag{A6}$$

while the process $c\bar{s}\to d\bar{u}+l^+l^+$ has to be considered separately:

$$|\mathcal{M}_{c\bar{s}\to d\bar{u}+l^+l^+}|^2=\left|\frac{V_{cd}V_{us}}{V_{ud}^2}\mathcal{M}_{u\bar{d}\to d\bar{u}+l^+l^+}^{(WW\text{-fusion})}+\frac{V_{cs}}{V_{ud}}\mathcal{M}_{u\bar{d}\to d\bar{u}+l^+l^+}^{(u\bar{d}\text{-annihil})}\right|^2. \tag{A7}$$

$\underline{c\bar{d}}$ collisions: the processes $c\bar{d}\to[s\bar{c},d\bar{u},d\bar{c}]+l^+l^+$ can be factorized as

$$\begin{aligned}|\mathcal{M}_{c\bar{d}\text{-initiated}}|^2&=\left(\frac{V_{cd}}{V_{ud}}\right)^2\left[1+\left|\frac{V_{cd}}{V_{ud}}\right|^2+\left|\frac{V_{cs}}{V_{ud}}\right|^2\right]\times|\mathcal{M}_{u\bar{d}\to d\bar{u}+l^+l^+}|^2,\\&=\left[1+\left|\frac{V_{cd}}{V_{cs}}\right|^2+\left|\frac{V_{ud}}{V_{cs}}\right|^2\right]\times|\mathcal{M}_{c\bar{s}\to d\bar{c}+l^+l^+}|^2;\end{aligned} \tag{A8}$$

and the process $c\bar{d}\to s\bar{u}+l^+l^+$ has to be considered separately:

$$|\mathcal{M}_{c\bar{d}\to s\bar{u}+l^+l^+}|^2=\left|\frac{V_{cs}}{V_{ud}}\mathcal{M}^{(\underline{WW}\text{-fusion})}_{u\bar{d}\to d\bar{u}+l^+l^+}+\frac{V_{cd}V_{us}}{V_{ud}^2}\mathcal{M}^{(\underline{u\bar{d}}\text{-annihil})}_{u\bar{d}\to d\bar{u}+l^+l^+}\right|^2. \quad \text{(A9)}$$

Finally the amplitude of the process $uc\to ds+l^+l^+$ although weighted by only one u-quark distribution function contains a graph multiplied by diagonal elements of the CKM matrix ($\propto V_{ud}^2V_{cs}^2$) see Eq. (22) and turns out to yield a contribution comparable to that of the $q\bar{q}'$ subprocesses described above (see Fig. 5). The contributions discussed in Eqs. (A4)–(A9) are reported in Fig. 5 together with the process $uc\to ds+l^+l^+$. The sum of these subprocesses accounts for about 10% of the total σ_1 reported in Fig. 4.

APPENDIX B: SQUARE OF AMPLITUDES

For the convenience of the reader interested in numerical applications the square of the amplitudes of the WW fusion mechanism is given here expressed in terms of the particles' momenta scalar products. In the numerical calculations it has been checked that one obtains an agreement of 1 part in 10^5 between this way of calculating the square of the amplitudes and the other consisting in writing down complex amplitudes and numerically taking the square of the absolute value.

Defining the quantities $K_i(i=1,2,3)$ by

$$\sum_{\text{pol}}|\mathcal{M}_i|^2=512\,\mathcal{F}^{(i)}_{CKM}\mathcal{K}^2K_i, \quad \text{(B1)}$$

they are explicitly (i) $U_iU_j\to D_kD_l+l^+l^+$:

$$\begin{aligned}K_i=p_a\cdot p_b\Bigg(&+A^2\,p_a\cdot p_c\,p_b\cdot p_d\left[+\frac{p_a\cdot p_e\,p_b\cdot p_f}{C^2}+\frac{p_a\cdot p_f\,p_b\cdot p_e}{D^2}-\frac{L(p_a,p_e,p_b,p_f)}{CD}\right]\\&+B^2\,p_a\cdot p_d\,p_b\cdot p_c\left[+\frac{p_a\cdot p_e\,p_b\cdot p_f}{E^2}+\frac{p_a\cdot p_f\,p_b\cdot p_e}{F^2}-\frac{L(p_a,p_e,p_b,p_f)}{EF}\right]\\&-AB\left\{L(p_a,p_c,p_b,p_d)\left[\frac{p_a\cdot p_e\,p_b\cdot p_f}{CE}+\frac{p_a\cdot p_f\,p_b\cdot p_e}{DF}-\frac{1}{2}L(p_a,p_e,p_b,p_f)\left(\frac{1}{CF}+\frac{1}{DE}\right)\right]\right.\\&\left.-\frac{1}{2}\epsilon(p_a,p_b,p_c,p_d)\cdot\epsilon(p_a,p_b,p_e,p_f)\left(\frac{1}{CF}-\frac{1}{DE}\right)\right\}\Bigg);\end{aligned} \quad \text{(B2)}$$

(ii) $U_i\bar{D}_j\to D_k\bar{U}_l+l^+l^+$:

$$K_{ii}=p_a\cdot p_d\,p_b\cdot p_d\,p_c\cdot p_a\,A^2\left\{+\frac{p_e\cdot p_a\,p_f\cdot p_d}{C^2}+\frac{p_f\cdot p_a\,p_e\cdot p_d}{D^2}-\frac{L(p_e,p_a,p_f,p_d)}{CD}\right\}; \quad \text{(B3)}$$

(iii) $\bar{D}_i\bar{D}_j\to\bar{U}_k\bar{U}_l+l^+l^+$:

$$\begin{aligned}K_{iii}=p_c\cdot p_d\Bigg\{&+A^2\,p_a\cdot p_c\,p_b\cdot p_d\left[+\frac{p_c\cdot p_e\,p_f\cdot p_d}{C^2}+\frac{p_c\cdot p_f\,p_e\cdot p_d}{D^2}-\frac{L(p_c,p_e,p_d,p_f)}{CD}\right]\\&+B^2\,p_a\cdot p_d\,p_b\cdot p_c\left[+\frac{p_c\cdot p_f\,p_e\cdot p_d}{E^2}+\frac{p_c\cdot p_e\,p_f\cdot p_d}{F^2}-\frac{L(p_c,p_e,p_d,p_f)}{EF}\right]\\&-AB\left\{L(p_a,p_c,p_b,p_d)\left[\frac{p_c\cdot p_e\,p_f\cdot p_d}{CF}+\frac{p_c\cdot p_f\,p_e\cdot p_d}{ED}-\frac{1}{2}L(p_e,p_c,p_f,p_d)\left(\frac{1}{CE}+\frac{1}{DF}\right)\right]\right.\\&\left.-\frac{1}{2}\epsilon(p_a,p_b,p_c,p_d)\cdot\epsilon(p_e,p_f,p_c,p_d)\left(\frac{1}{CE}-\frac{1}{DF}\right)\right\}\Bigg\}\end{aligned} \quad \text{(B4)}$$

with $L(p_a,p_b,p_c,p_d)=p_a\cdot p_b\,p_c\cdot p_d+p_a\cdot p_d\,p_b\cdot p_c-p_a\cdot p_c\,p_b\cdot p_d$.

[1] C. Rubbia, Rev. Mod. Phys. **57**, 699 (1985).

[2] S. Weinberg, Phys. Rev. Lett. **19**, 1264 (1967); A. Salam, in *Elementary Particle Theory: Relativistic Groups and Analyticity (Nobel Symposium No. 8)*, edited by Svartholm (Almqvist and Forlag, Stockholm, 1968).

[3] Proceedings of the First International Conference on *Particle Physics Beyond the Standard Model*, Castle Ringberg, Germany, 1997; *Beyond the Desert 1997*, edited by H. V. Klapdor-Kleingrothaus and H. Päs (Institute of Physics, Bristol, 1998).

[4] J. C. Pati and A. Salam, Phys. Rev. D **10**, 275 (1974).

[5] J. L. Hewett and T. G. Rizzo, Phys. Rep. **183**, 193 (1989).

[6] R. Barbieri, R. N. Mohapatra, and A. Masiero, Phys. Lett. **105B**, 369 (1981); **107B**, 455(E) (1981).

[7] For a review and further references see, for example, W. C. Haxton and G. J. Stephenson, Prog. Part. Nucl. Phys. **12**, 409 (1984).

[8] H. V. Klapdor-Kleingrothaus, in Ref. [3], p. 485. In Eq. (10) the most recent $\beta\beta_{0\nu}$ bound has been used as reported in L. Baudis *et al.*, Phys. Rev. Lett. **83**, 41 (1999); H. V. Klapdor-Kleingrothaus, hep-ph/9901021. In *Trento 1998, Lepton and Baryon Number Violation* 251-301. Proceedings of the International Symposium On Lepton And Baryon Number Violation, 1998, Trento, Italy, edited by H. V. Klapdor-Kleingrothaus and I. V. Krivosheina (IOP, Bristol, 1999), p. 760.

[9] Proceedings of the International Workshop *Double Beta Decay and Related Topics* held at the European Centre for Theoretical Studies (ECT), Trento, Italy, 1995, edited by H. V. Klapdor-Kleingrothaus and S. Stoica (World Scientific, Singapore, 1996).

[10] M. Hirsch, H. V. Klapdor-Kleingrothaus, and S. G. Kovalenko, Phys. Lett. B **352**, 1 (1995); Phys. Rev. Lett. **75**, 17 (1995); Phys. Rev. D **53**, 1329 (1996).

[11] M. Hirsch, H. V. Klapdor-Kleingrothaus, and O. Panella, Phys. Lett. B **374**, 7 (1996).

[12] M. Hirsch, H. V. Klapdor-Kleingrothaus, and S. G. Kovalenko, Phys. Rev. D **54**, 4207 (1996); Phys. Lett. B **378**, 17 (1996).

[13] O. Panella and Y. N. Srivastava, Phys. Rev. D **52**, 5308 (1995).

[14] O. Panella, in Proceedings of the Trento workshop, see Ref. [9].

[15] O. Panella, C. Carimalo, Y. N. Srivastava, and A. Widom, Phys. Rev. D **56**, 5766 (1997).

[16] O. Panella, C. Carimalo, Y. N. Srivastava, and A. Widom, in *Beyond the Desert 1997*, Ref. [3].

[17] Wai-Yee Keung and Goran Senjanović, Phys. Rev. Lett. **50**, 1427 (1983).

[18] Amitava Datta, Manoranjan Guchait, and D. P. Roy, Phys. Rev. D **47**, 961 (1993).

[19] D. A. Dicus, D. D. Karatas, and P. Roy, Phys. Rev. D **44**, 2033 (1991).

[20] O. Panella, Ph.D. thesis, Northeastern University, 1991; O. Panella, Y. N. Srivastava, and A. Widom, Northeastern University report, 1991 (unpublished).

[21] S. Dawson, Nucl. Phys. **B249**, 42 (1985).

[22] H. Terazawa, Y. Chikashige, and K. Akama, Phys. Rev. D **15**, 480 (1977); H. Harari, Phys. Lett. **86B**, 83 (1979); H. Fritzsch and G. Mandelbaum, *ibid.* **102B**, 319 (1981); O. Greenberg and J. Schuler, *ibid.* **99B**, 339 (1981); R. Barbieri, R. N. Mohapatra, and A. Masiero, *ibid.* **105B**, 369 (1981); for further references see, for example, H. Harari, Phys. Rep. **104**, 159 (1984); I. A. D'Souza and C. S. Kalman, *Preons, Models of Leptons, Quarks and Gauge Bosons as Composite Objects* (World Scientific, Singapore, 1992).

[23] Particle Data Group, C. Caso *et al.*, Euro. Phys. J. C **3**, 1 (1998; 1999 off-year partial update for the 2000 edition available on the PDG WWW pages (URL http://pdg.lbl.gov/).

[24] N. Cabibbo, L. Maiani, and Y. Srivastava, Phys. Lett. **139B**, 459 (1984).

[25] A. De Rujula, L. Maiani, and R. Petronzio, Phys. Lett. **140B**, 253 (1984).

[26] U. Baur, I. Hinchliffe, and D. Zeppenfeld, Int. J. Mod. Phys. A **2**, 1285 (1987).

[27] J. C. Pati and A. Salam, Phys. Rev. Lett. **31**, 661 (1973); R. N. Mohapatra and J. C. Pati, Phys. Rev. D **11**, 566 (1975); R. N. Mohapatra, *Unification and Supersymmetry* (Springer, New York, 1986).

[28] DELPHI Collaboration, Report No. CERN-EP/196, 1998.

[29] ALEPH Collaboration, R. Barate *et al.*, Eur. Phys. J. C **4**, 571 (1998).

[30] ALEPH Collaboration, R. Barate *et al.*, Phys. Lett. B **429**, 201 (1998).

[31] ZEUS Collaboration, Breitweg *et al.*, Z. Phys. C **76**, 631 (1997).

[32] A. Djouadi, J. Ng, and T. G. Rizzo (unpublished); in *Electroweak Symmetry Breaking and Beyond the Standard Model*, edited by T. Barklow, S. Dawson, H. E. Haber, and S. Siegrist (World Scientific, Singapore, in press), hep-ph/9504210; U. Baur, M. Spira, and P. M. Zerwas, Phys. Rev. D **42**, 815 (1990).

[33] R. Kleiss and W. J. Stirling, Nucl. Phys. **B262**, 235 (1985).

[34] J. F. Owens, Phys. Lett. B **266**, 126 (1991).

[35] G. P. Lepage, J. Comput. Phys. **27**, 192 (1978).

[36] CTEQ Collaboration, J. Botts *et al.*, Phys. Lett. B **304**, 159 (1993).

[37] A. D. Martin, R. G. Roberts, and W. J. Stirling, Phys. Lett. B **354**, 155 (1995).

[38] M. Glück, E. Reya, and A. Vogt, Z. Phys. C **67**, 433 (1995).

[39] CMS Collaboration, L. Servoli (private communication).

[40] J. Hellmig and H. V. Klapdor-Kleingrothaus, Z. Phys. A **359**, 351 (1997).

[41] M. Hirsch (private communication); see also H. V. Klapdor-Kleingrothaus and M. Hirsch, Z. Phys. A **359**, 361 (1997).

[42] The DAΦNE Project Team, ''DAΦNE, Status and Plans,'' Proceedings of PAC95, 1995.

[43] The KLOE Collaboration, ''Status of the KLOE experiment,'' LNF-97/033, 1997.